Polymer Chemistry

PAPER

View Article Online
View Journal | View Issue

Cite this: *Polym. Chem.*, 2019, **10**, 2282

Self-catalysed folding of single chain nanoparticles (SCNPs) by NHC-mediated intramolecular benzoin condensation†

Sofiem Garmendia,[a,b,c,d] Andrew P. Dove,[d] Daniel Taton[a,b] and Rachel K. O'Reilly*[d]

Received 29th January 2019,
Accepted 22nd March 2019

DOI: 10.1039/c9py00149b

rsc.li/polymers

A self-catalysed folding strategy to form single chain nanoparticles (SCNPs) was developed *via* an intramolecular *N*-heterocyclic carbene (NHC)-mediated benzoin condensation. Benzaldehyde, styrene and benzimidazolium chloride units were randomly incorporated into a poly(ionic liquid)-based (PIL) copolymer precursor by reversible addition–fragmentation chain transfer (RAFT) copolymerisation. Post-chemical modification of this linear precursor by insertion of a non-innocent acetate counter-anion into the benzimidazolium moieties conferred thermolatent catalytic behaviour owing to the equilibrium between benzimidazolium acetate units and corresponding NHC ones. Upon heating, catalytically active NHCs allowed the formation of benzoin-type intramolecular cross-links, thus folding linear chains into SCNPs. NHC moieties became deactivated after cooling to room temperature, which enabled easy isolation and purification of the covalently and intramolecularly cross-linked SCNPs. Importantly, the latent NHC moieties were proven to retain their catalytic activity when arranged into SCNPs as evidenced through their reactivation by simple heating. The catalytic activity of these SCNPs was further confirmed by implementing another NHC-organocatalysed reaction, namely, transesterification reaction between vinyl acetate and benzyl alcohol. This work represents the first example of catalysis by a parent linear precursor which drives its own folding and remains catalytically active.

Introduction

Single-chain nanoparticles (SCNPs) have recently emerged as versatile soft nano-objects with unique characteristics, that make them suitable in an array of applications, such as nanomedicine,[1,2] bioapplications (bioimaging, drug delivery),[3,4] or catalysis.[5–7] SCNPs consist of single polymer chains that are cross-linked through intramolecular bonding, in an attempt to mimic the unique properties of natural biomacromolecules (*e.g.* polypeptides, DNA, enzymes).[8–13] In this context, synthetic enzymatic mimics that utilise polymer backbones present a number of opportunities for preparing efficient catalysts, by controlling key properties such as polymer solubility,[14] increased accessibility to a larger library of substrates,[15] increased turnover frequency (TOF),[16] recycling,[17–19] or supporting organic/metallic catalysts on a soluble polymeric support.[20–24] The most common strategy to prepare SCNPs is based on the design of a linear single chain precursor that features pendant functionalities to facilitate folding through the formation of intramolecular cross-links following exposure to an external stimulus (*e.g.* temperature, solvent, UV-irradiation), or addition of external reagents.[13,25–27] After covalent and/or non-covalent cross-linking, the SCNPs may be used as nanoreactors. However, the catalytic ability of the parent linear precursor has not been so far exploited as a driving force for its own folding. Here, new insight is brought to this field through immobilisation of both the reactive functionality and the catalyst onto the same linear copolymer precursor, enabling triggering through a self-catalysed folding as a novel route to SCNPs (Scheme 1).

One possible obstacle to the folding process lies in the orthogonality between reactive functionalities and the catalyst. We therefore turned to the use of a copoly(ionic liquid) (coPIL) precursor, PILs representing modular polymeric platforms where different orthogonal functionalities can be introduced, thanks to the broad selection of monomeric ionic liquids.[28–30]

[a]*Laboratoire de Chimie des Polymères Organiques, Université de Bordeaux IPB-ENSCBP, F-33607 Pessac Cedex, France*
[b]*Laboratoire de Chimie des Polymères Organiques Centre National de la Recherche Scientifique, 16 Avenue Pey-Berland, F-33607 Pessac Cedex, France*
[c]*Department of Chemistry, University of Warwick, Coventry, CV4 7AL, UK*
[d]*School of Chemistry, The University of Birmingham, Edgbaston, Birmingham, B15 2TT, UK. E-mail: R.OReilly@bham.ac.uk*

†Electronic supplementary information (ESI) available. See DOI: 10.1039/c9py00149b

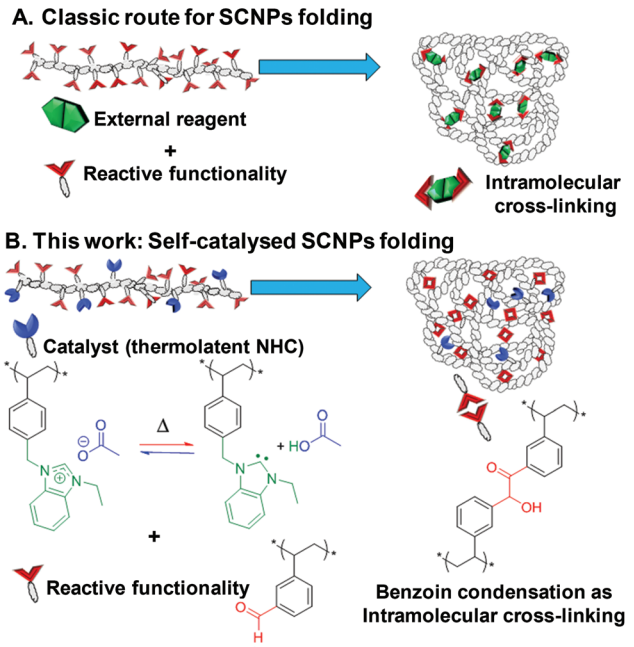

Scheme 1 Strategies to conduct SCNP synthesis for use as catalytic nanoreactors. (A) Classic route involving the addition of external reagents to induce chain folding. (B) Self-catalysed SCNPs folding mediated by supported thermally latent NHC precatalysts.

In particular imidazolium-based ILs are known as versatile precursors of *N*-heterocyclic carbenes (NHCs), which can be activated *in situ* for instance by means of solvent change or upon heating among other triggers. More specifically, imidazolium-based precursors featuring a slightly basic counter-anion, *e.g.* hydrogen carbonate,[31] acetate,[32] sebacate[33] or benzoate,[19] can autonomously generate NHCs, *i.e.* without the need for any external reagent, owing to the deprotonation of the C2-position by the basic anion. Installation of the latter is straightforward as it can be achieved one step by simple anion-metathesis (= anion exchange reaction). Synthesis of imidazolium-type coPILs bearing such anions provides a convenient strategy to immobilize latent NHCs onto a polymeric support, which can be catalytically turned on and off simply upon heating. NHCs have gained increasing popularity in the last three decades, not only as ligands for transition metals, but also as true organocatalysts for numerous molecular and macromolecular transformations.[34–37] The so-called benzoin condensation is an emblematic NHC-catalysed carbon–carbon bond-forming reaction occurring by self-condensation of two aldehyde substrates forming a β-keto alcohol with no by-product.[38,39] By introducing both latent aldehyde-type units and benzimidazolium acetate units as site-isolated latent NHCs into the same copolymer chain, we reasoned that intramolecular benzoin condensation of supported benzaldehydes could be triggered by simple heating under dilute solution, causing the single copolymer chain to fold through the formation of benzoin-type cross-links. This inherent thermal-latency would be further harnessed by cooling/deactivating the masked supported NHCs after folding, to isolate the resulting SCNPs. These could be further used as nanoreactors to mediate another NHC-catalysed reaction, namely, transesterification between benzyl alcohol and vinyl acetate. Herein, we thus report a novel self-catalysed folding strategy to SCNPs, forming intramolecular covalent cross-links of benzoin-type. Of particular interest, the resulting SCNPs remains catalytically active. By immobilizing for the first time both the catalytic species and the substrates onto the same single copolymer chain, the synthetic strategy we describe here further expands the scope of SCNPs.

Experimental

Materials

Benzimidazole (≥95%), 4-vinylbenzyl chloride (90%), ethyl bromide (99%), 3-vinylbenzaldehyde, acetonitrile and 2-cyano-2-propyl benzodithioate (≥97%) were obtained from Sigma-Aldrich and used as received. 3-Vinylbenzaldehyde, potassium acetate and $MgSO_4$ were obtained from Sigma-Aldrich and used as purchased. Azobis(2-methylpropionitrile) (AIBN, 99%) was received from Sigma-Aldrich and was purified by recrystallisation from methanol. Styrene, dimethylformamide (DMF), vinyl acetate, benzyl alcohol and carbon disulfide (CS_2) were dried over CaH_2 and distilled prior to use. Monomer **1** and molecular model catalyst **8** were prepared as reported elsewhere.[14,19,33] Tetrahydrofuran (THF) was distilled over Na/benzophenone. Ethyl acetate (99.7%, Aldrich) was used without further purification. Methanol was distilled over metallic Na prior to use. "Standard Grade Regenerated Cellulose Dialysis Membranes (Spectra/Por6) Pre-wetted RC tubing" from SpectrumLab with a molecular weight cut off (MWCO) of 3.5 kDa were used after cleaning with pure water.

Characterisation

^{1}H NMR, ^{13}C NMR spectra were recorded using a Bruker AC-400 spectrometer in appropriate deuterated DMSO-d_6. All ^{13}C measurements were performed at 298 K on a Bruker Avance III 400 spectrometer operating at 100.7 MHz and equipped with a 5 mm Bruker multinuclear direct cryoprobe. All DOSY (Diffusion Ordered Spectroscopy) measurements were performed at 298 K on a Bruker Avance III HD 400 spectrometer operating at 400.33 MHz and containing a 5 mm Bruker multinuclear *z*-gradient direct cryoprobe-head capable of producing gradients in the *z* direction with strength 53.5 G cm^{-1}. For each sample, 3 mg was dissolved in 0.4 μl of DMSO-d_6 for internal lock and spinning was used to minimise convection effects. DOSY spectra were acquired with the ledbpgp2s pulse program from Bruker Topspin software. The duration of the pulse gradients and the diffusion time were adjusted in order to obtain full attenuation of the signals at 95% of maximum gradient strength. The values were 2.0 ms for the duration of the gradient pulses and 300 ms for the diffusion time. The gradients strength was linearly incremented in 16 steps from 5% to 95% of the maximum gradient strength. A

delay of 3 s between echoes was used. The data were processed using 8192 points in the F2 dimension and 256 points in the F1 dimension with the Bruker Topspin software. Field gradient calibration was accomplished at 25 °C using the self-diffusion coefficient of H_2O + D_2O at 19.0 × 10^{-10} m^2 s^{-1}. DMF soluble polymers were first solubilised in concentrations of 1 mg mL^{-1} and their masses were determined by size exclusion chromatography (SEC) in DMF (5 mM $NH_4^+BF_4^-$) at 50 °C using a UV detector (Varian) calibrated with polystyrene standards. Analysis was performed using a three-column set of TSK gel TOSOH (G4000, G3000, G2000 with pore sizes 20, 75, 200 Å respectively, connected in series). A Bruker spectrometer was used for ATR-FTIR analysis. Hydrodynamic diameters (D_h) and size distributions of SCNPs were determined by DLS on a Malvern Zetasizer Nano ZS operating at 20 °C with a 4 M_w He–Ne 633 nm laser module. Samples were filtered through a 0.2 μm PTFE filter prior to measurement and quartz cuvettes were used. Measurements were made at a detection angle of 173° (back scattering), and the data analysed using Malvern DTS 7.12 software, using the multiple narrow modes setting. All measurements were made in triplicate, with 4 runs per measurement. TEM analysis was performed on a JEOL 2011 (LaB_6) microscope operating at 200 keV, equipped with a GATAN UltraScan 1000 digital camera. Conventional bright field conditions were lacey carbon-coated copper grids (Agar Scientific, 400 mesh, S116-4) coated with a thin layer of graphene oxide.[40] SCNPs solutions were diluted to 1 mg mL^{-1} in MeOH before 4 μL of each sample were drop-deposited onto the graphene oxide coated grids, blotted immediately and allowed to air dry. Subsequent staining was applied using uranyl acetate to enhance the contrast. Images were analysed using Image J software, and 20 particles were measured to produce a mean and standard deviation for the particle size (D_{av}).

Synthesis

Synthesis of linear copolymer 2. 2-Cyano-2-propyl benzodithioate (43 mg, 0.19 mmol) as a chain transfer agent (CTA), styrene (2.4 mL, 23.6 mmol), 4-vinylbenzylethylbenzimidazolium chloride (1.18 g, 3.93 mmol), 3-vinylbenzaldehyde (1.5 mL, 11.8 mmol) and AIBN (31 mg, 0.19 mmol) were dissolved in 12 mL of DMF. The solution was purged with nitrogen for 30 min and stirred for 12 h at 80 °C. The as-obtained copolymer was purified by dialysis against methanol (1 L × 2 every 24 h, MWCO 3.5 kDa membrane) and the solvent was removed under reduced pressure, yielding copolymer **2** as a pink powder (1.6 g, yield = 31%). ^{1}H NMR (DMSO-d_6): δ = 10.9–10.1 (br, 1H, N═*CH*–N), 9.9–9.6 (br, 3H, *H*–CO–), 8.2–6.1 (br, 53.1 H, Ar–), 5.9–5.5 (br, 2H, Ar–*CH*$_2$–N), 4.7–4.5 (br, 2H, N–*CH*$_2$–CH_3, 2.2–0.9 (br, 30.2 H, backbone, CH_2–*CH*$_3$) (Fig. S1†). ^{13}C NMR (DMSO-d_6): δ = 193.1, 147.6–143.9, 142.7, 136.6–124.8, 114.2, 80.1, 42.9, 14.4 (Fig. S2†). SEC analysis: $Đ_M$ = 1.2; M_n = 11.9 kDa.

Synthesis of linear copolymer 3. Copolymer **2** (1 g, 0.095 mmol) was dissolved in 12 mL of methanol and 3 mL of chloroform in a round-bottom flask. Potassium acetate (0.15 g, 1.15 mmol) was added and the reaction mixture was stirred overnight at room temperature. The solution was filtered and purified by dialysis against methanol/ethanol (75 : 25, 1 L × 2 every 24 h, MWCO 3.5 kDa membrane). The solvent was removed under reduced pressure, yielding copolymer **3** as a yellow powder (0.93 g, yield = 92%). ^{1}H NMR (DMSO-d_6): δ = 10.5–9.6 (br, 4H, *H*–CO–, N═*CH*–N), 8.2–6.1 (br, 53.1 H, Ar–), 5.8–5.5 (br, 2H, Ar–*CH*$_2$–N), 4.7–4.5 (br, 2H, N–*CH*$_2$–CH_3, 2.2–0.9 (br, 36.4 H, backbone, O═C–*CH*$_3$, CH_2–*CH*$_3$) (Fig. S3†). ^{13}C NMR (DMSO-d_6): δ = 193.1, 176.6, 147.6–143.9, 143.7, 136.6–124.8, 114.2, 80.1, 59.8, 42.9, 24.4, 14.4 (Fig. S4†).

Synthesis of linear copolymer 4. Copolymer **3** (80 mg, 0.008 mmol) was first azeotropically dried in THF. The sample was then heated at 80 °C for 24 h in THF (3 mL) in presence of CS_2 (0.6 mL). The solvent and excess of CS_2 were removed under reduced pressure, yielding copolymer **4** as a red viscous oil (yield > 95%). ^{1}H NMR (DMSO-d_6): δ = 12.2–12.0 (br, 0.5 H, –COO*H*), 10.5–9.6 (br, 1H, *H*–CO–), 8.2–6.1 (br, 34.2 H, Ar–*H*), 5.8–5.4 (br, 2H, Ar–*CH*$_2$–N), 4.4–4.2 (br, 2H, N–*CH*$_2$–CH_3, 2.2–0.2 (br, 32.6 H, backbone, HOOC–*CH*$_3$, –CH_2–*CH*$_3$) (Fig. S5†). ^{13}C NMR (DMSO-d_6): δ = 224.1, 193.1, 174.4, 153.1, 147.6–143.9, 141.3, 136.6–124.8, 114.2, 110.1, 71.1, 52.3, 24.4, 13.7 (Fig. S6†).

Synthesis of SCNP 5. Copolymer **3** (150 mg, 0.015 mol) was dissolved in 150 mL of dry THF and heated to 80 °C in a 1 L Schlenk flask for 48 h. The solvent was removed under reduced pressure and the resulting material was dialysed against methanol (1 L × 2 every 24 h, MWCO 3.5 kDa membrane) producing SCNP **5** (130 mg, yield = 87%). ^{1}H NMR (DMSO-d_6): δ = 12.0–11.8 (br, 1H, N═*CH*–N), 10.1–9.7 (br, 1.2 H, O═C–*H*), 8.3–5.8 (br, 47.5 H, Ar–H), 5.4 (s, 0.3 H, O═C–C*H*OH–Ar), 4.2 (s, 0.25 H, O═C–CHO*H*–Ar), 4.05 (s, 0.15 H, N–CH_2–CH_3), 2.2–0.2 (br, 50.2 H, backbone, O═C–*CH*$_3$, –CH_2–*CH*$_3$) (Fig. S7†). ^{13}C NMR (DMSO-d_6): δ = 179.3, 172.6, 153.1 147.6–143.9, 140.0, 132.1–122.6, 97.6, 80.7, 67.9, 53.3, 42.9, 24.4, 14.4 (Fig. S8†). SEC analysis: $Đ_M$ = 1.2; M_n = 10.8 kDa.

Synthesis of SCNP 6. SCNP **5** (35 mg, 0.003 mmol) was dissolved in THF (2 mL) in presence of a large excess of CS_2 (0.4 mL) in a Schlenk tube for 24 h at 80 °C. Yield > 95%. ^{1}H NMR (DMSO-d_6): δ = 12.9–12.3 (br, 0.4 H, –COO*H*), 10.4–9.6 (br, 1H, *H*–CO–), 8.3–5.9 (br, 40.8 H, Ar–*H*),5.4 (s, 0.2 H, O═C–*CH*OH–Ar), 5.2–5.0 (br, 0.5 H, Ar–*CH*$_2$–N), 4.4–4.2 (br, 0.4 H, O═C–CH*OH*–Ar) 2.3–0.2 (br, 51.2 H, backbone, HOOC–*CH*$_3$, –CH_2–*CH*$_3$) (Fig. S14†). ^{13}C NMR (DMSO-d_6): δ = 193.3, 168.8, 153.1, 152.0, 147.6–143.9, 139.9, 135.1–122.6, 109.6, 97.6, 80.7, 67.9, 42.9, 24.4, 19.4 (Fig. S13†).

Synthesis of the model polymer 7. 2-Cyano-2-propyl benzodithioate CTA (30 mg, 0.13 mmol), styrene (2.34 mL, 20.4 mmol) and monomer **1** (0.68 g, 2.26 mmol) were added to a 20 mL glass tube. Methanol (12 mL) was added and the suspension was allowed to stir for 10 min until a homogenous solution was obtained. AIBN (27 mg, 0.11 mmol) was added to the methanolic solution under dry nitrogen at room temperature. After mixing and purging the solution with dry nitrogen, the glass tube was sealed and placed at 80 °C in an oil bath for 16 h. After this time, 52% conversion was reached, as evi-

denced by ^{1}H NMR spectroscopy. The reaction was then quenched by cooling the solution to room temperature. The crude copolymer was purified by dialysis against methanol (1 L × 2 every 24 h, MWCO 3.5 kDa membrane). The obtained copolymer (0.9 g) was solubilised in methanol and subjected to anion exchange by adding potassium acetate (0.65 g, 10 eq.) to the solution and then further dialysed against methanol (1 L × 2 every 24 h) using a 3.5 kDa MWCO dialysis membrane. Yield = 40%. ^{1}H NMR (DMSO-d_6): δ = 11.5–10.2 (br, 1H, N=*CH*–N), 8.2–6.1 (br, 30.1 H, Ar–), 5.9–5.5 (br, 2H, Ar–*CH*$_2$–N), 4.7–4.5 (br, 2H, N–*CH*$_2$–CH$_3$), 2.2–0.9 (br, 10.6 H, backbone, O=C–CH$_3$, CH$_2$–*CH*$_3$) (Fig. S16†). SEC analysis: $Đ_M$ = 1.1; M_n = 12.7 kDa (Fig. S17†).

General procedure for the transesterification reaction. In a 10 mL glass tube, different catalysts were first azeotropically dried using distilled THF. Dry THF was then added, maintaining a reference catalyst concentration of 0.015 mmol mL^{-1} referred to benzimidazolium moieties. The solution was stirred, and previously distilled benzyl alcohol (1 eq.) and vinyl acetate (1.2 eq.) were added under nitrogen. The resulting mixture was stirred under nitrogen at 80 °C for 2 h. The reaction kinetics were monitored by extracting aliquots every 15 min and calculating the conversion by comparing the integral value of the signal due to the –CH$_2$– group of benzyl alcohol (*d*, 2H, 4.5 ppm) to that of the –CH$_2$– benzyl acetate signal (*d*, 2H, 5 ppm) by ^{1}H NMR spectroscopy in DMSO-d_6 (Fig. S18–S29†).

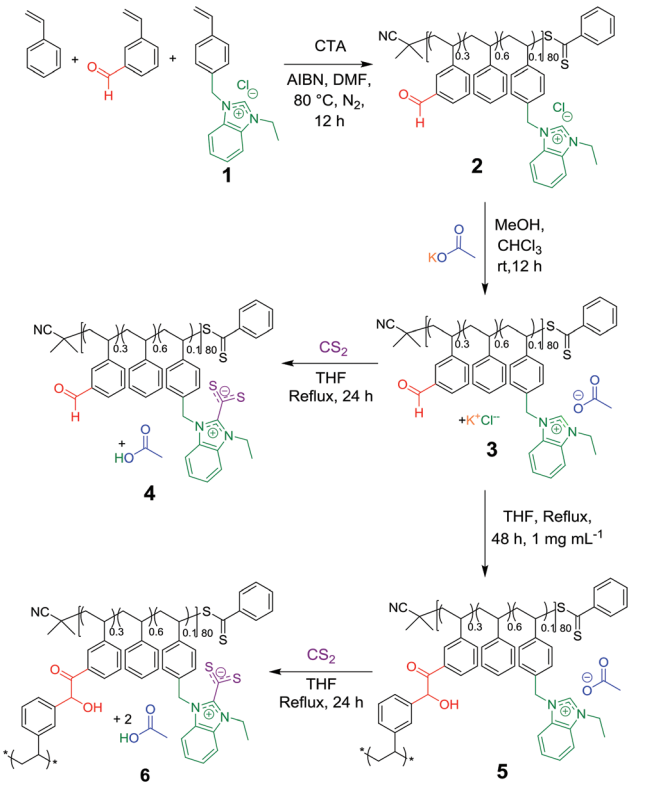

Scheme 2 Synthetic route to functional linear copolymer **3** and subsequent self-catalysed folding step leading to catalytically active SCNP **5**. The NHC-CS$_2$ functionalised versions of both linear precursor (**4**) and obtained SCNP (**6**) as well as corresponding active NHC intermediates are also represented.

Results and discussion

Synthesis of catalytically active SCNPs

The linear statistical single chain precursor was devised to be constituted of three distinct monomer units, namely, deriving from benzaldehyde, benzimidazolium and styrene functionalities (Scheme 2). As emphasised above, benzimidazolium chloride moieties served as NHC precursors, benzaldehyde as reactive substrate both being immobilised onto the coPIL backbone, while styrene units would play the role as spacers to facilitate easier accessibility of the NHC catalyst to the reactive functionalities, also conferring some hydrophobicity to the copolymer backbone.

As depicted in Scheme 2, the IL monomer, namely, 4-vinylbenzylethylbenzimidazolium chloride **1** was synthesised following an established procedure.[14,19,33] Copolymerisation of **1** with 3-vinylbenzaldehyde and styrene was achieved *via* the reversible addition fragmentation chain transfer (RAFT) process in DMF, using AIBN as a radical source and 2-cyano-2-propyl benzodithioate as the RAFT agent. A [Monomer(s)]/[CTA]/[AIBN] ratio of 98/1/1 was targeted. The reaction was carried out for 12 h at 80 °C, reaching *ca.* 40% conversion. The structure of the resulting linear coPIL **2** was authenticated by ^{1}H NMR spectroscopy. In particular, the proportion of the different monomer units within the backbone structure could be determined by relative integration of the characteristic signals of each monomer obtained by ^{1}H NMR spectroscopy (Fig. S1†). Briefly, the intensity of signals corresponding to the aldehyde proton was compared to the *N*-alkylated moieties of benzimidazolium chloride, *i.e.* benzyl-*CH*$_2$–N at 5.4 ppm and br. N–*CH*$_2$–CH$_3$ at 4.6 ppm, and the aromatic region at 6–8 ppm, corresponding to the number of styrene units. This calculation gave an average composition of 48 styrene units, 8 units of **1** and 24 units of benzaldehyde. Therefore, the calculated molecular weight for copolymer **2** was found equal to ~10.5 kg mol^{-1}, that was, slightly smaller than the value delivered by SEC in DMF of 11.9 kg mol^{-1}.

The benzimidazolium chloride functionality was then subjected to an anion exchange, substituting the acetate anion for the chloride in one step and thus affording a latent NHC pre-catalyst.[41] This metathesis reaction was carried out at room temperature in dry methanol in presence of KOAc, yielding copolymer **3** (Fig. S3 and S4†). This was confirmed first by the appearance of a new signal corresponding to acetate –CH$_3$ protons at *ca.* 1 ppm in ^{1}H NMR analysis and the presence of the same acetate carbonyl signal at 176.6 ppm in ^{13}C NMR spectroscopy. This strategy enables the easy handling and storage of the coPIL precursor **3** in an inactive state at low temperature.[21,32,42,43]

We first examined the latent NHC-like behaviour of coPIL **3** *via* a simple chemical postmodification consisting in the reac-

tion between benzimidazolium acetate units with an excess of carbon disulfide (CS_2). Upon heating in THF this reaction mixture for 24 h, polymer-supported NHCs thus released NHCs from **3** are trapped, forming a red solution characteristic of a NHC-CS_2 adduct (= copolybetaine **4**). This was evidenced by the appearance of diagnostic signals in the ^{13}C NMR spectrum at 224.1 ppm and 153.1 ppm corresponding to C_{2imi} and CS_2^-, respectively (Fig. S6†).[31,44]

This reaction test thus allowed us to confirm the crucial role of acetate anion in supplying copoly(NHC)s from the linear coPIL precursor **3** upon heating. The self-catalysed folding based on the intramolecular benzoin condensation of benzaldehyde units could then be investigated. To this end, a solution of coPIL **3** was heated to 80 °C in THF at 1 mg mL^{-1} concentration for 48 h. The folding process generating SCNP **5** constituted of benzoin covalent cross-links was evaluated by ^1H and ^{13}C NMR spectroscopy, size exclusion chromatography (SEC), dynamic light scattering (DLS), transmission electron microscopy (TEM), diffusion-ordered spectroscopy (DOSY) NMR and Fourier-transform infrared spectroscopy (FTIR). Characteristic signals corresponding to the newly formed benzoin moieties were clearly detected in the ^1H NMR spectrum, namely, at 5.4 ppm (H from the chiral benzoin carbon) and at 4.2 ppm (–OH from the same chiral carbon; Fig. S7†). ^{13}C NMR analysis also revealed the presence of both a newly formed carbonyl signal at 179.3 ppm and the –CH– benzoin carbon at 80.7 ppm (Fig. S8†). Formation of benzoin-type cross-links was further evidenced by HSQC spectroscopy (Fig. S9†) correlating the –CH– of benzoin moieties to the corresponding chiral carbon atom. Furthermore, FT-IR spectroscopy showed both the appearance of the benzoin –OH group at 3300 cm^{-1}, as well as the broadening of the carbonyl vibration signal at 1700 cm^{-1}, due to the presence of the acetate (counter-anion), ketone (benzoin) and residual aldehyde (Fig. S10†). Self-folding was also demonstrated by a decrease in the hydrodynamic diameter of the as-obtained SCNPs, according to different analytical techniques, as summarised in Fig. 1. Firstly, a decrease in the apparent molecular weight was noted by SEC, compared to the linear precursor **2** (Fig. 1A) due to compaction by intramolecular cross-linking upon forming SCNP **5**. DLS performed in THF at 20 °C revealed a slight decrease in hydrodynamic diameter (D_H), from 7.5 nm to 6.1 nm (Fig. 1B; see Fig. S11† for the range 20–80 °C). In addition, dry-state TEM analysis confirmed the presence of spherical nanoparticles corresponding to SCNP **5** with an average diameter of *ca.* 4.5 nm (Fig. 1C). Finally, DOSY NMR spectroscopy in DMSO-d_6 showed a reduction in diameter after the self-catalysed benzoin condensation step, with a diameter of 2.3 nm calculated for SCNP **5**, whilst a value of 6.6 nm was obtained for the linear precursor **2** (Fig. S12†). All these results are consistent with a compaction due to self-catalysed folding step formation benzoin-type cross-links.

As SCNPs **5** thus formed still contains benzimidazolium acetate units, they were in turn evaluated as masked NHCs. This was first achieved through their post-functionalisation by insertion of CS_2, generating polybetaine **6**. Thus, the reaction mixture in THF turned orange upon heating **5** in the presence of CS_2 after 24 h. The characteristic signal of functionalised C_{2imi} at 153.1 ppm (Fig. S13†) was again present in the ^{13}C NMR spectrum of **6**, although it was hardly detected likely because of the confined environment provided by SCNP **6**. In contrast, the COOH proton of the acetic acid by-product released during the functionalisation step was detected in the ^1H NMR spectrum, appearing at 12.5 ppm (Fig. S14†). Formation of polybetaine **6** was further confirmed by FT-IR spectroscopy with the appearance of the asymmetric vibration of CS_2^- at 1030 cm^{-1} (Fig. S15†). These results highlight that thermally latent NHC units remain active after the folding step.

The activity of SCNPs **5** was next tested in another NHC-mediated organocatalysis application, namely, the transesterification reaction between vinyl acetate and benzyl alcohol. This was first achieved in THF using 1 eq. of benzyl alcohol and a slight excess of vinyl acetate (1.2 eq.), in presence of 1 mol% of SCNP-supported masked NHCs **5**. Under such conditions, only 6% of benzyl alcohol was converted into benzyl acetate after 2 h (run 1; Table 1). Further optimisation using a loading of the catalytic SCNP **6** equal to 5 and 10 mol%, whilst maintaining the concentration of reagents, allowed us to increase the conversion to 43% and up to 69% respectively (runs 2 and 3). For a comparison purpose, SCNP **5** was compared to a linear statistical coPIL analogue **7** constituted of benzimidazolium acetate and styrene units, *i.e.* poly(styrene-

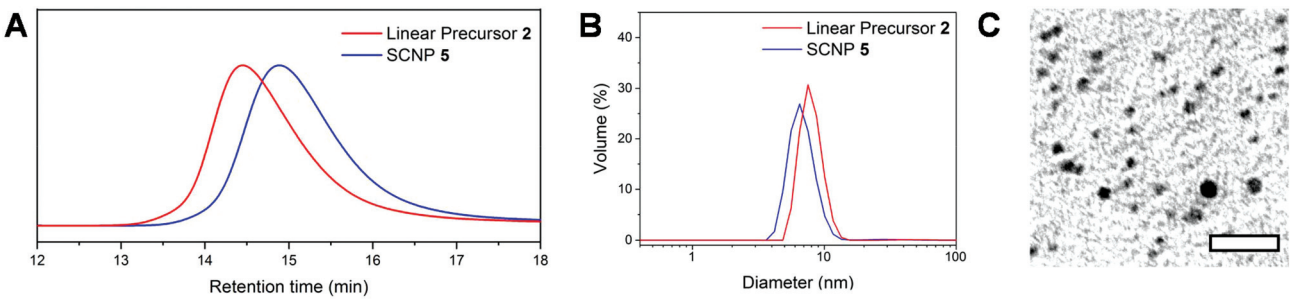

Fig. 1 (A) SEC traces (in DMF with 10 mM NH_4BF_4) of SCNP **5** (blue line) obtained *via* intramolecular cross-linking of coPIL **2** (red line) by self-catalysis (UV detector). (B) DLS analysis of coPIL **2** (red line) and SCNP **5** (blue line) diameters at 20 °C distributed by volume in THF (conc. 1 mg mL^{-1}). (C) TEM images of SCNP **5** (conc. 1 mg mL^{-1} in methanol) stained with uranyl acetate. Scale bar = 20 nm.

Table 1 Transesterification between benzyl alcohol and vinyl acetate under different reaction conditions using masked NHC-containing SCNPs and control experiments

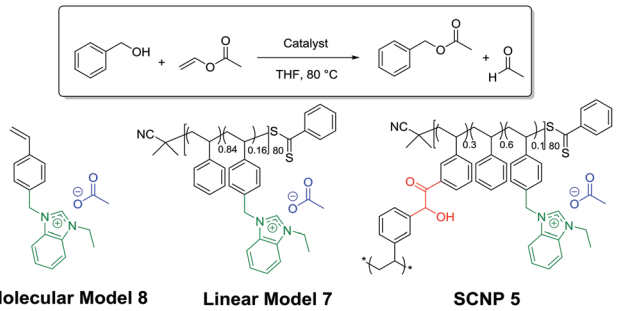

Molecular Model 8 **Linear Model 7** **SCNP 5**

Run	Catalyst	Cat. (mol%)	Conv.[a] (%)
1	SCNP **5**[b]	1	6
2	SCNP **5**	5	43
3	SCNP **5**	10	69[c]
4	**7**[d]	1	42
5	**7**	5	97
6	**7**	10	>99
7	**8**[e]	1	96
8	**8**	5	93
9	**8**	10	>99
10	SCNP **5**[f]	10	0
11	Copolymer **2**	10	0
12	Potassium acetate	10	<2
13	—[g]	0	0

[a] The reaction was run for 2 h and conversions were calculated by ^{1}H NMR spectroscopy by comparing the integral value of the –CH_2– benzyl alcohol signal (*d*, 2H, 4.5 ppm) to that of the –CH_2– benzyl acetate signal (*d*, 2H, 5 ppm) by ^{1}H NMR spectroscopy in DMSO-d_6 (Fig. S18–29). [b] THF was used as solvent and dried under Na/benzophenone prior to use in each catalytic run being 0.015 mmol mL^{-1} reference catalyst concentration referred to benzimidazolium at 10 mol%. [c] The conversion barely increased duplicating the reaction time up to 4 h of reaction obtaining *ca.* 70% conversion. [d] Linear model 7 containing randomly ordered spacers and active monomer units in a 84/16 ratio. [e] Active monomer based molecular model **8**. [f] The same conditions as in run 1 were used running the experiment at rt instead of 80 °C. [g] This reaction was performed only using benzyl alcohol (1 eq.) and vinyl acetate (1.2 eq.) for 2 h at 80 °C. The results correspond to the average value obtained after two different runs for each reaction.

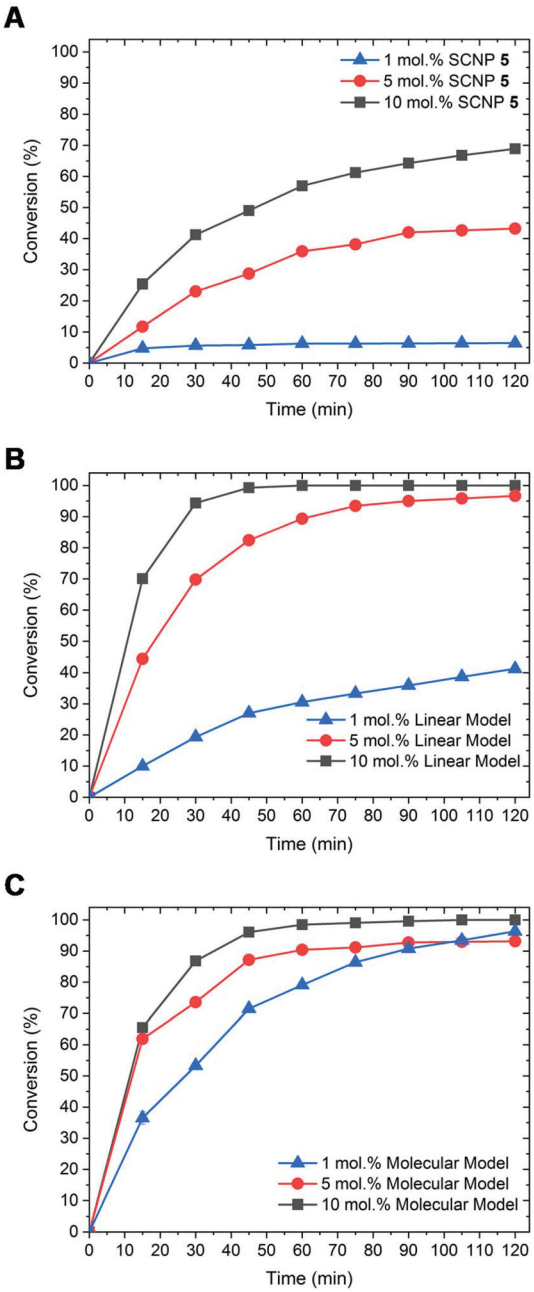

Fig. 2 Kinetics for transesterification reaction at 1 mol% (blue line), 5 mol% (red line) and 10 mol% (black line) using (A) SCNP **5**, (B) **7** and (C) **8** as catalysts.

co-4-vinylbenzylethylbenzimidazolium acetate) and to the 4-vinylbenzimidazole ethylimidazolium acetate monomer **8**, serving as molecular model. Both the molecular and macromolecular models were assessed for the transesterification reaction under the same catalysis conditions as SCNP **5**. Faster catalysis kinetics was observed from coPIL **7** compared to SCNP **5** (Fig. 2B), providing faster kinetics and higher conversions upon increasing the pre-catalyst loading (almost quantitative conversion was noted for 5 and 10 mol% *vs.* 42% for 1 mol% runs 5, 6 and run 4, respectively). In comparison, almost quantitative conversions were obtained using 1, 5 and 10 mol% catalyst loading of the molecular model after only 2 h (runs 7–9).

In light of these comparative investigations of the three different catalytic systems (SCNP **5** *vs.* coPIL **7** and monomer **8**), higher conversions and faster rates observed with both the molecular and the linear coPIL models suggest that the microenvironment provided by SCNP **5** somehow restricts the catalytic activity of supported-NHCs relatively to both the linear and molecular models.[5,45–48] As expected, no organocatalytic activity was noted at room temperature, while the transesterified reaction product formed upon heating, demonstrating the thermal latency of SCNP **5** (run 3 *vs.* run 10). Despite the fact that SCNP **5** did not improve the catalytic performance of the transesterification reaction, it has been shown that the cata-

lytic activity of the NHC is retained within the compact core of the 3D-SCNP.

Conclusions

In this work, the modularity of PIL chemistry has been further exploited to design individual linear copolymer chains by RAFT, combining thermally latent and autonomous NHC behaviour, *i.e.* in absence of any external reagent, and the capability to self-catalyse some substrate units immobilized on these chains. These unique features can be exploited to achieve SCNPs by self-NHC-organocatalysed folding of the individual chains, as evidenced by different analytical techniques, including SEC, TEM, DLS and DOSY NMR. To this end, 3-vinylbenzaldehyde, styrene and 4-vinylbenzylethylbenzimidazolium chloride were randomly copolymerised using the RAFT process, resulting in a well-defined but catalytically inactive coPIL support. Installation of a slightly basic acetate counterion by anion metathesis imparts the catalytic activity and thermally latent behaviour to the coPIL precursor. The self-catalysed folding process lead to the formation of SCNPs occurs by the formation of covalent cross-links through the benzoin condensation of benzaldehyde moieties. The as-obtained SCNPs retain their NHC behaviour, as demonstrated not only through the trapping of CS_2, but also by the possibility to further catalyse the transesterification reaction between vinyl acetate and benzyl alcohol. Comparison with both a molecular and a linear coPIL catalyst homologues show however that the confined environment provided by the SCNPs does not improve the organocatalytic performance. Efforts to tune the catalytic environment of the SCNPs, by varying the cross-linking density, is currently in progress. Overall, this study highlights the versatility of thermally-latent NHC catalysts, demonstrating their use as a novel trigger for the folding of catalytically active SCNP nanoreactors.

Conflicts of interest

There are no conflicts to declare.

Acknowledgements

This work was supported by EU through project SUSPOL-EJD 642671. We thank Anne-Laure Wirotius at the University of Bordeaux for DOSY NMR spectroscopy and Stefan B. Lawrenson from the University of Birmingham for contributing to the preparation of the manuscript.

Notes and references

1 R. Gracia, M. Marradi, G. Salerno, R. Pérez-Nicado, A. Pérez-San Vicente, D. Dupin, J. Rodriguez, I. Loinaz, F. Chiodo and C. Nativi, *ACS Macro Lett.*, 2018, **7**, 196–200.
2 T.-K. Nguyen, S. J. Lam, K. K. K. Ho, N. Kumar, G. G. Qiao, S. Egan, C. Boyer and E. H. H. Wong, *ACS Infect. Dis.*, 2017, **3**, 237–248.
3 Y. Liu, S. Pujals, P. J. M. Stals, T. Paulöhrl, S. I. Presolski, E. W. Meijer, L. Albertazzi and A. R. A. Palmans, *J. Am. Chem. Soc.*, 2018, **140**, 3423–3433.
4 I. Perez-Baena, I. Loinaz, D. Padro, I. García, H. J. Grande and I. Odriozola, *J. Mater. Chem.*, 2010, **20**, 6916.
5 H. Rothfuss, N. D. Knöfel, P. W. Roesky and C. Barner-Kowollik, *J. Am. Chem. Soc.*, 2018, **140**, 5875–5881.
6 J. Rubio-Cervilla, E. González and J. Pomposo, *Nanomaterials*, 2017, **7**, 341.
7 J. Rubio-Cervilla, E. González and J. A. Pomposo, in *Single-Chain Polymer Nanoparticles*, ed. J. A. Pomposo, Wiley-VCH Verlag GmbH & Co. KGaA, Weinheim, Germany, 2017, pp. 341–388.
8 J. A. Pomposo, I. Perez-Baena, F. Lo Verso, A. J. Moreno, A. Arbe and J. Colmenero, *ACS Macro Lett.*, 2014, **3**, 767–772.
9 A. Latorre-Sánchez and J. A. Pomposo, *Polym. Int.*, 2016, **65**, 855–860.
10 M. Ouchi, N. Badi, J.-F. Lutz and M. Sawamoto, *Nat. Chem.*, 2011, **3**, 917–924.
11 A. M. Hanlon, C. K. Lyon and E. B. Berda, *Macromolecules*, 2016, **49**, 2–14.
12 O. Altintas and C. Barner-Kowollik, *Macromol. Rapid Commun.*, 2016, **37**, 29–46.
13 S. Mavila, O. Eivgi, I. Berkovich and N. G. Lemcoff, *Chem. Rev.*, 2016, **116**, 878–961.
14 R. Lambert, A.-L. Wirotius, S. Garmendia, P. Berto, J. Vignolle and D. Taton, *Polym. Chem.*, 2018, **9**, 3199–3204.
15 Y. Bai, X. Feng, H. Xing, Y. Xu, B. K. Kim, N. Baig, T. Zhou, A. A. Gewirth, Y. Lu, E. Oldfield and S. C. Zimmerman, *J. Am. Chem. Soc.*, 2016, **138**, 11077–11080.
16 M. Artar, T. Terashima, M. Sawamoto, E. W. Meijer and A. R. A. Palmans, *J. Polym. Sci., Part A: Polym. Chem.*, 2014, **52**, 12–20.
17 Y. Azuma, T. Terashima and M. Sawamoto, *ACS Macro Lett.*, 2017, **6**, 830–835.
18 N. D. Knöfel, H. Rothfuss, J. Willenbacher, C. Barner-Kowollik and P. W. Roesky, *Angew. Chem., Int. Ed.*, 2017, **56**, 4950–4954.
19 S. Garmendia, A. P. Dove, D. Taton and R. K. O'Reilly, *Polym. Chem.*, 2018, **9**, 5286–5294.
20 M. Artar, E. R. J. Souren, T. Terashima, E. W. Meijer and A. R. A. Palmans, *ACS Macro Lett.*, 2015, **4**, 1099–1103.
21 R. Lambert, A.-L. Wirotius and D. Taton, *ACS Macro Lett.*, 2017, **6**, 489–494.
22 J. Willenbacher, O. Altintas, V. Trouillet, N. Knofel, M. J. Monteiro, P. W. Roesky and C. Barner-Kowollik, *Polym. Chem.*, 2015, **6**, 4358–4365.
23 A. Sanchez-Sanchez, A. Arbe, J. Colmenero and J. A. Pomposo, *ACS Macro Lett.*, 2014, **3**, 439–443.
24 J. De-La-Cuesta, I. Asenjo-Sanz, A. Latorre-Sánchez, E. González, D. E. Martínez-Tong and J. A. Pomposo, *Eur. Polym. J.*, 2018, **109**, 447–452.

25 I. Berkovich, V. Kobernik, S. Guidone and N. G. Lemcoff, in *Single-Chain Polymer Nanoparticles*, ed. J. A. Pomposo, Wiley-VCH Verlag GmbH & Co. KGaA, Weinheim, Germany, 2017, pp. 217–257.
26 H. Frisch, J. P. Menzel, F. R. Bloesser, D. E. Marschner, K. Mundsinger and C. Barner-Kowollik, *J. Am. Chem. Soc.*, 2018, **140**, 9551–9557.
27 S. Basasoro, M. Gonzalez-Burgos, A. J. Moreno, F. L. Verso, A. Arbe, J. Colmenero and J. A. Pomposo, *Macromol. Rapid Commun.*, 2016, **37**, 1060–1065.
28 *Applications of Ionic Liquids in Polymer Science and Technology*, ed. D. Mecerreyes, Springer Berlin Heidelberg, Berlin, Heidelberg, 2015.
29 J. Yuan, D. Mecerreyes and M. Antonietti, *Prog. Polym. Sci.*, 2013, **38**, 1009–1036.
30 A. Eftekhari and T. Saito, *Eur. Polym. J.*, 2017, **90**, 245–272.
31 M. Fèvre, J. Pinaud, A. Leteneur, Y. Gnanou, J. Vignolle, D. Taton, K. Miqueu and J.-M. Sotiropoulos, *J. Am. Chem. Soc.*, 2012, **134**, 6776–6784.
32 R. Lambert, P. Coupillaud, A.-L. Wirotius, J. Vignolle and D. Taton, *Macromol. Rapid Commun.*, 2016, **37**, 1143–1149.
33 S. Garmendia, R. Lambert, A.-L. Wirotius, J. Vignolle, A. P. Dove, R. K. O'Reilly and D. Taton, *Eur. Polym. J.*, 2018, **107**, 82–88.
34 M. Fevre, J. Pinaud, Y. Gnanou, J. Vignolle and D. Taton, *Chem. Soc. Rev.*, 2013, **42**, 2142.
35 S. Naumann and A. P. Dove, *Polym. Chem.*, 2015, **6**, 3185–3200.
36 D. M. Flanigan, F. Romanov-Michailidis, N. A. White and T. Rovis, *Chem. Rev.*, 2015, **115**, 9307–9387.
37 W. N. Ottou, H. Sardon, D. Mecerreyes, J. Vignolle and D. Taton, *Prog. Polym. Sci.*, 2016, **56**, 64–115.
38 R. S. Menon, A. T. Biju and V. Nair, *Beilstein J. Org. Chem.*, 2016, **12**, 444–461.
39 M. Alrayyani and O. Š. Miljanić, *Chem. Commun.*, 2018, **54**, 11989–11997.
40 M. W. P. van de Put, J. P. Patterson, P. H. H. Bomans, N. R. Wilson, H. Friedrich, R. A. T. M. van Benthem, G. de With, R. K. O'Reilly and N. A. J. M. Sommerdijk, *Soft Matter*, 2015, **11**, 1265–1270.
41 S. Naumann and M. R. Buchmeiser, *Catal. Sci. Technol.*, 2014, **4**, 2466.
42 O. Holloczki, D. Gerhard, K. Massone, L. Szarvas, B. Nimeth, T. Veszprimi and L. Nyulaszi, *New J. Chem.*, 2010, **34**, 3004.
43 G. Gurau, H. Rodriguez, S. P. Kelley, P. Janiczek, R. S. Kalb and R. D. Rogers, *Angew. Chem., Int. Ed.*, 2011, **50**, 12024–12026.
44 L. Delaude, *Eur. J. Inorg. Chem.*, 2009, **2009**, 1681–1699.
45 J. A. Pomposo, J. Rubio-Cervilla, A. J. Moreno, F. Lo Verso, P. Bacova, A. Arbe and J. Colmenero, *Macromolecules*, 2017, **50**, 1732–1739.
46 P. Cotanda, N. Petzetakis and R. K. O'Reilly, *MRS Commun.*, 2012, **2**, 119–126.
47 A. D. Ievins, X. Wang, A. O. Moughton, J. Skey and R. K. O'Reilly, *Macromolecules*, 2008, **41**, 2998–3006.
48 A. Lu, P. Cotanda, J. P. Patterson, D. A. Longbottom and R. K. O'Reilly, *Chem. Commun.*, 2012, **48**, 9699.